# Micro-polar and second-order homogenization of periodic masonry

Andrea Bacigalupo[1], Luigi Gambarotta[1]

[1]*Department of Civil, Environmental and Architectural Engineering, University of Genoa, Italy*
*E-mail*: *bacigalupo @dicat.unige.it, gambarotta@dicat.unige.it*

*Keywords:* non-local continuum, computational homogenization, masonry.

SUMMARY. Micro-polar and second order homogenization procedures for periodic elastic masonry are implemented to include geometric and material length scales in the constitutive equation. By the solution of the RVE equilibrium problems with properly prescribed boundary conditions the orthotropic elastic moduli of the higher order continua are obtained on the basis of an enhanced Hill–Mandel condition. A shear layer problem is analysed and the results from the heterogeneous models are compared with those ones obtained by the homogenization procedures; the second-order homogenization appears to provide better results in comparison to the micro-polar homogenization.

## 1 INTRODUCTION

Classical homogenization methods have been proposed and applied to derive average properties of periodic masonry based on the properties of the constituents (brick/blocks, mortar) and their arrangements (see Mistler *et al* [1]). In their standard form, however, these methods fail to include the scale of the heterogeneous masonry material in the resulting constitutive equations. To appreciate the influence on the overall response of the size of masonry units and of high stress and strain gradients and to prevent pathological localizations arising from the assumption of strain-softening constitutive equations for the masonry components higher order or multi-field equivalent continua appear to be necessary.

Overall constitutive equations of a two-dimensional micropolar continuum for periodic masonry have been obtained in [2-4] through a homogenization procedure based on an idealization of the masonry as an assemblage of rigid blocks represented as a Lagrangian systems composed of bodies interacting through linear elastic interfaces. Although these approaches provide overall elastic moduli that depend in closed form on the mechanical and geometric characteristics of the components, the rigid blocks assumption seems rather restrictive in many cases when the brick compliance is comparable to the mortar one's. To include this effect a micro-polar computational homogenization of a representative unit cell (RVE) extracted from the periodic masonry made up of elastic brick units and mortar joints has been proposed in [5], where the rotational dof of the micropolar homogenised continuum has been identified through a heuristic evaluation of the mean local rotation of the brick units.

Higher-order gradient theories for periodic, linear elastic media have been developed using an asymptotic solution of the microstructural problem in [6-8]. A computational procedures has been developed in [9]; the application to matrix-inclusion composite showed that higher-order terms become more important as the stiffness contrast between inclusion and matrix increases. As observed in [9], the drawback of this approach, that provides a mathematically rigorous tool of higher-order modelling, is the computational burden.

Different homogenization approaches for higher-order continua have been derived by attributing some specific polynomial displacement fields to the unit cell to be added to an unknown displacement fluctuation field that makes the unit cell in equilibrium with proper boundary conditions. A couple-stress homogenization technique of periodic heterogeneous materials has been developed in [10,11], where the effects of boundary conditions on the representative volume element are analyzed and discussed. The Cosserat homogenization technique proposed in [12] has been extended to periodic masonry in [13] in order to analyse different masonry patterns that cannot be considered by the previous approaches. Here, the influence of the elastic mismatch between the components on the characteristic lengths of the equivalent orthotropic elastic continuum has been analyzed and validity limits of the homogenization procedure have been discussed.

Second order homogenization of periodic masonry seems to be an appealing alternative to the Cosserat homogenization. In fact, second order models do not involve independent rotational degrees of freedom, so reducing the complexity of the computational homogenization, and provide extensional characteristic lengths of the equivalent continuum. In the present paper, a second-order homogenization of periodic masonry is considered, in order to couple a classical continuum at the scale of the RVE with a second order continuum at the macroscale. According to [14] and [15] the macroscopic displacement gradient tensor and its gradient are used to prescribe the essential boundary conditions on the micro-displacement field in the RVE, here extended as generalized periodic boundary conditions. By the solution of the equilibrium problem of the RVE, the micro-displacement and micro-strain fields are evaluated and the orthotropic elastic moduli of the second order continuum are obtained on the basis of an enhanced Hill–Mandel condition.

An evaluation of the micro-polar and second-order homogenization techniques is carried out by a sensitivity analysis of the characteristic lengths of the non-local continua to the elastic compliances of the components. Moreover, a shear layer problem concerning a masonry wall is analysed and the numerical results from the heterogeneous models are compared with those ones obtained by homogenization procedures.

## 2 NON-LOCAL HOMOGENIZATION OF PERIODIC MASONRY

A brief outline of the homogenization procedures developed for periodic masonry is here presented with reference to the representative volume element shown in Fig. 1 extracted by a masonry wall. The bond pattern is characterized by vectors of periodicity $\mathbf{v}_1$, $\mathbf{v}_2$ and the brick units and the mortar joints are assumed linear elastic, so implying orthotropic constitutive equations for the homogenized continua. Let be the position of the center of RVE identified by vector $\mathbf{y}$ and the relative position with respect to this point of a point in RVE identified by vector $\mathbf{x}$. The displacement field $\mathbf{u}(\mathbf{x})$ in the heterogeneous RVE located at the reference origin ($\mathbf{y}=\mathbf{0}$) is assumed as the sum of two contributions $\mathbf{u}(\mathbf{x}) = \mathbf{u}^*(\mathbf{x}) + \tilde{\mathbf{u}}(\mathbf{x})$, being $\mathbf{u}^*(\mathbf{x})$ the truncated Taylor's series expansion

$$u_i^*(x_j) = \alpha_{ij} x_j + \frac{1}{2}\beta_{ijh} x_j x_h + \frac{1}{6}\gamma_{ijhk} x_j x_h x_k \tag{1}$$

and $\tilde{\mathbf{u}}(\mathbf{x})$ the microstructural displacement fluctuation field. Moreover, the displacement field $\tilde{\mathbf{u}}(\mathbf{x})$ is assumed periodic on the boundary $C$ of the RVE, i.e. $\tilde{\mathbf{u}}(\mathbf{x}_b + \mathbf{v}_i) = \tilde{\mathbf{u}}(\mathbf{x}_b)$ ($i$=1,2) at points $\mathbf{x}_b \in C$. As a consequence, the periodic boundary constraints on $C$ to be applied on the

displacement field $\mathbf{u}(\mathbf{x})$ take the form $\mathbf{u}(\mathbf{x}_b+\mathbf{v}_i)-\mathbf{u}(\mathbf{x}_b)=\mathbf{u}^*(\mathbf{x}_b+\mathbf{v}_i)-\mathbf{u}^*(\mathbf{x}_b)$, being the r.h.s. terms depending on the parameters $\alpha_{ij}$, $\beta_{ijh}$, $\gamma_{ijhk}$.

The macro strain and the macro rotation in the RVE are, respectively,

$$\overline{\varepsilon}_{ij}=\frac{1}{2A}\int_{\partial A}\left(u_i n_j+u_j n_i\right)\,da \quad , \quad \overline{\omega}_{21}=\frac{1}{2A}\int_{\partial A}\left(u_2 n_1-u_1 n_2\right)\,da \quad . \tag{2}$$

The first order homogenization procedure is obtained by assuming $\beta_{ijh}=\gamma_{ijhk}=0$ and based on the Hill-Mandel macro-homogeneity condition. The standard constitutive equations of elastic plane orthotropy involve four independent elastic moduli of orthotropy ($\overline{\sigma}_{ij}$ components of the mean stress tensor)

$$\overline{\sigma}_{ii}=C_{iihh}\overline{\varepsilon}_{hh} \qquad (i,h=1,2), \qquad \overline{\sigma}_{12}=C_{1212}2\overline{\varepsilon}_{12} \quad . \tag{3}$$

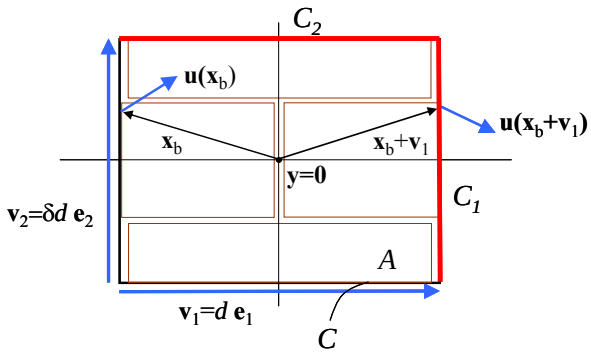


Fig. 1. RVE, vectors of periodicity, displacement at the boundary.

In case of Cosserat homogenization, according to the approach proposed in [7] and extended in [8] to periodic masonry, the macro-rotation and the relative macro-rotation in the RVE are, respectively,

$$\phi=\frac{1}{\tilde{J}_p}\int_A\left(\delta^2 u_2 x_1-u_1 x_2\right)da \quad , \quad \theta=\phi-\overline{\omega}_{21} \tag{4}$$

and depend on the displacement field in the RVE. The components of the curvature tensor are

$$k_i=\phi_{,i}=\frac{1}{\tilde{J}_p}\int_A\left(\delta^2 u_{2,i} x_1-u_{1,i} x_2\right)da \quad \text{(i=1,2)} \quad , \quad \text{with } \tilde{J}_p=\int_A\left(\delta^2 x_1^2-x_2^2\right)da \; . \tag{5}$$

Both the macro-rotation $\phi$ and the curvatures $k_1$ and $k_2$ are depending on some non-vanishing terms $\beta_{ijh}$ , $\gamma_{ijhk}$ . By an extension of the Hill-Mandel condition the elastic orthotropic constitutive equations involving eight independent elastic moduli for the centro-symmetric material are obtained

$$\begin{aligned} &\overline{\sigma}_{ii} = \overline{\tau}_{ii} = C_{iihh}\,\overline{\varepsilon}_{hh} \qquad (i,h=1,2) \\ &\overline{\tau}_{ij} = \overline{C}_{ijhk}\,\overline{\eta}_{hk} \qquad (i,j=1,2;\ h,k=1,2;\ i\neq j,\ h\neq k) \\ &m_i = Y_i\ k_i \qquad (i,h=1,2) \end{aligned} \tag{6}$$

being $\overline{\eta}_{12} = \overline{\varepsilon}_{12} - \theta$ , $\overline{\eta}_{21} = \overline{\varepsilon}_{21} + \theta$ , $\overline{\tau}_{ij}$ the stress tensor component, with symmetric part $\overline{\tau}_{(ij)} = \overline{\sigma}_{ij}$ , and $m_i$ component of the couple-stress tensor, respectively.

In second order homogenization the in-plane component of the macro-strain tensor and the macro-rotation tensor are defined in equation (2) and a higher order strain tensor $\chi_{ijh}$ is considered, with symmetric $\chi_{(ij)h}$ and antisymmetric $\chi_{[21]i}$ parts, depending on the displacement field on the boundary of the RVE in the form

$$\chi_{ijh}\mathrm{J}_{hh} + \frac{1}{2}\delta_{hj}\chi_{ipp}\mathrm{J}_{pp} = \int_C u_i x_h n_j\, ds \quad , \ \text{with}\ \mathrm{J}_{ii} = \int_A x_i^2\, da \quad , \ i,\ j,\ h = 1,2 \quad . \tag{7}$$

In this case the homogenization is obtained by imposing displacement conditions on the boundary *C* of the RVE according to the Taylor's expansion in (1) truncated to the second order $\left(\gamma_{ijhk}=0\right)$; the periodic boundary condition on the displacement field in the RVE have to be generalized according to [9] by imposing the mean of the microstructural displacement fluctuation field on each side of the RVE to be vanishing

$$\int_{C^r} \tilde{u}_i\ ds = \int_{C^r} \left(u_i - \alpha_{ij}x_j + \beta_{ijh}x_j x_h\right)\ ds = 0 \quad , \quad r = 1,2 \quad , \tag{8}$$

being $C^1$ and $C^2$ the vertical and horizontal part of the RVE boundary, respectively, as shown in Fig. 1. By imposing the Hill-Mandel condition the orthotropic constitutive equations are obtained, combining the first order equations (3) and two uncoupled groups of equations, each having the form

$$\boldsymbol{\mu}_i = \mathbf{S}^i\boldsymbol{\chi}_i \qquad (i=1,2) \quad . \tag{9}$$

The vectors $\boldsymbol{\chi}_1 = \left\{\chi_{222} \quad \chi_{(12)1} \quad k_1 = \chi_{[21]1}\right\}^T$ and $\boldsymbol{\chi}_2 = \left\{\chi_{111} \quad \chi_{(12)2} \quad k_2 = \chi_{[21]2}\right\}^T$ collect the components of the second order strain tensor, respectively, and $\boldsymbol{\mu}_1 = \left\{\mu_{222} \quad \mu_{(12)1} \quad m_1 = \mu_{[21]1}\right\}^T$ and $\boldsymbol{\mu}_2 = \left\{\mu_{111} \quad \mu_{(12)2} \quad m_2 = \mu_{[21]2}\right\}^T$ collect the corresponding components of the second order stress tensor. Moreover, the stress tensor

$$\overline{\tau}_{ij} = \overline{\sigma}_{ij} - \mu_{(ij)h,h} - \mu_{[ij]h,h} \tag{10}$$

depends on the symmetric stress tensor and on the second order stress tensor. As a consequence sixteen independent elastic moduli are defined: the four moduli of first order (Cauchy) model and the moduli $S^i_{hk}$ in (9).

For the special case of couple-stresses continuum model or Koiter model, a reduced number of elastic moduli is involved collecting the first order Cauchy moduli (3) and the constitutive equations $m_i = Y_i\ k_i = S^i_{33}\ k_i$ ($i$=1,2) related to the components of the curvature tensor and of the couple-stress tensor; here, six independent moduli have to be identified for the RVE.

## 3 NUMERICAL APPLICATION AND COMPARISONS

In order to evaluate the homogenization procedures summarized in the previous section, a periodic masonry made of plain bricks arranged in a running bond pattern has been analysed with reference to the RVE shown in Fig. 1. The brick dimensions are 25cm x 14cm with a thickness of 1cm; the mortar thickness is 1cm ($d$=26cm, $\delta = 14/26$). Bricks and mortar are assumed to be isotropic; for the mortar the Young Modulus $Em$ = 500MPa is assumed and the Poisson ratio is assumed $\nu_m = \nu_b = 0.1$ for both the constituents. The elastic moduli of the homogeneous equivalent continuum have been evaluated for increasing values of the Young modulus of the bricks ($Eb$=10-$10^3 Em$) in order to appreciate the effect of mismatch in the elastic moduli of the constituents. The elastic moduli obtained by the standard first-order (Cauchy) homogenization are given in Table 1, while the moduli of the equivalent Cosserat continuum in (6) are given in Table 2. Finally, the elastic moduli $S^1_{hk}$ and $S^2_{hk}$ introduced in (9) for the second order continuum are given in Table 3.

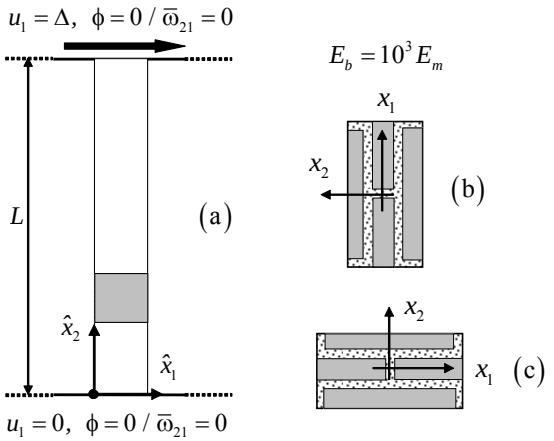


Fig. 2. BSL model (a); vertical brick layers VBL (b); horizontal brick layers HBL (c).

To evaluate the capability of the different homogenization procedure, the macroscopic boundary shear layer problem (BSL) is analysed numerically with reference to the vertical column shown in Fig. 2.a. Two cases are considered corresponding to different orientations of the RVE: in

the former case the brick layers are vertical (Fig. 2.b), while the latter case refers to horizontal brick layers (Fig.2.c). In both cases the height $L$ of the column is $n$=10 times the corresponding size of the RVE ($Lb$=260cm, $Lc$=140cm). The bottom edge is fixed, while a horizontal displacement $\Delta = L/100$ is prescribed on the top edge; the rotations at the bottom and the top edges are restrained (homogeneous Cosserat model $\phi = 0$ ; second order models $\overline{\omega}_{12} = 0$ ).

In Fig. 3 the diagrams of the macro-rotation and the horizontal displacement along the BSL model evaluated by assuming a homogeneous Cosserat continuum are compared with the corresponding generalized displacements of portions of the heterogeneous model located at each RVE (the macro-rotation is evaluated by equation (4.1)). In the case of VBL model a good agreement is obtained in the results, while in case of horizontal brick layers (HBL) the Cosserat model does not appear to provide acceptable results. In fact, the results by the FEM analysis of the heterogeneous model show that in case of HBL the width of the boundary layer is negligible in comparison to the case VBL. Better results are obtained if the second order homogenization is applied, as shown by the diagrams in Fig. 4.

| $E_b$ | $C_{1111}$ (Mpa) | $C_{2222}$ (Mpa) | $C_{1122}$ (Mpa) | $C_{1212}$ (Mpa) |
|---|---|---|---|---|
| $10E_m$ | 3.466E+03 | 2.154E+03 | 1.990E+02 | 9.080E+02 |
| $10^2 E_m$ | 1.213E+04 | 3.271E+03 | 1.907E+02 | 1.369E+03 |
| $10^3 E_m$ | 1.645E+04 | 3.453E+03 | 1.369E+02 | 1.467E+03 |

Table 1. Elastic moduli: first order (Cauchy) homogenization.

| $E_b$ | $\overline{C}_{1212}$ (Mpa) | $\overline{C}_{2121}$ (Mpa) | $\overline{C}_{1221}$ (Mpa) | $Y_1$ (N) | $Y_2$ (N) |
|---|---|---|---|---|---|
| $10E_m$ | 7.143E+03 | 4.461E+03 | -3.876E+03 | 5.816E+06 | 1.180E+07 |
| $10^2 E_m$ | 2.674E+04 | 1.385E+04 | -1.662E+04 | 2.429E+07 | 2.813E+07 |
| $10^3 E_m$ | 1.941E+05 | 9.719E+04 | -1.346E+05 | 1.002E+08 | 1.491E+08 |

Table 2. Elastic moduli: Cosserat homogenization. (Equation (6)).

| $E_b$ | $S^1_{11}$ (N) | $S^1_{22}$ (N) | $S^1_{33} = Y_1$ (N) | $S^1_{12}$ (N) | $S^1_{13}$ (N) | $S^1_{23}$ (N) |
|---|---|---|---|---|---|---|
| $10E_m$ | 4.120E+05 | 2.670E+07 | 6.360E+06 | -2.895E+06 | 5.313E+04 | -6.727E+06 |
| $10^2 E_m$ | 8.803E+05 | 1.127E+08 | 4.714E+07 | -7.789E+06 | 1.717E+06 | -5.898E+07 |
| $10^3 E_m$ | 1.325E+06 | 4.252E+08 | 2.914E+08 | -1.427E+07 | 5.129E+06 | -3.268E+08 |
| | $S^2_{11}$ (N) | $S^2_{22}$ (N) | $S^2_{33} = Y_2$ (N) | $S^2_{12}$ (N) | $S^2_{13}$ (N) | $S^2_{23}$ (N) |
| $10E_m$ | 9.082E+06 | 1.505E+07 | 1.271E+07 | -4.650E+06 | 6.164E+05 | 1.236E+07 |
| $10^2 E_m$ | 1.810E+07 | 3.886E+07 | 3.310E+07 | -1.021E+07 | 2.821E+05 | 3.294E+07 |
| $10^3 E_m$ | 2.025E+07 | 1.855E+08 | 1.787E+08 | -1.167E+07 | 7.399E+04 | 1.787E+08 |

Table 3. Elastic moduli: second order homogenization (Equation (9)).

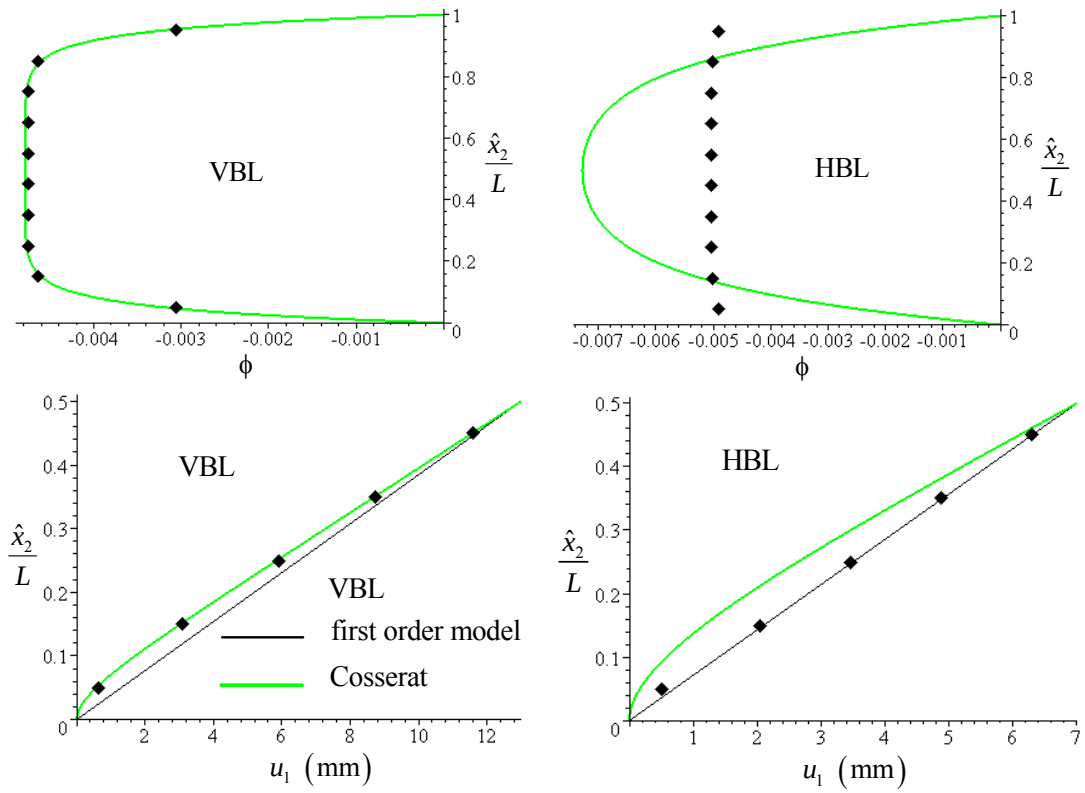


Fig. 3. BSL model: macro rotation and horizontal displacement at the RVEs from the heterogeneous model (diamonds) compared with the macro-rotation field in the homogeneous Cosserat model (continuous line).

This circumstance can be synthetically explained if the characteristic lengths of the homogeneous models are considered. Here, the shearing characteristic lengths of the Cosserat continuum ( $\lambda_1^{\mathrm{C}}, \lambda_2^{\mathrm{C}}$ ), Couple-stresses continuum ( $\lambda_1^{\mathrm{CS}}, \lambda_2^{\mathrm{CS}}$ ) and second-order continuum ( $\lambda_{Sh-1}^{2nd}$, $\lambda_{Sh-2}^{2nd}$ ) are

$$\lambda_1^{\mathrm{C}} = \sqrt{\frac{\overline{C}_{2121} Y_1}{\overline{C}_{1212}\overline{C}_{2121} - \overline{C}_{1221}{}^2}}, \quad \lambda_2^{\mathrm{C}} = \sqrt{\frac{\overline{C}_{1212} Y_2}{\overline{C}_{1212}\overline{C}_{2121} - \overline{C}_{1221}{}^2}}, \quad \lambda_1^{\mathrm{CS}} = \frac{1}{2}\sqrt{\frac{S_{33}^1}{C_{1212}}}, \quad \lambda_2^{\mathrm{CS}} = \frac{1}{2}\sqrt{\frac{S_{33}^2}{C_{1212}}},$$
$$\lambda_{Sh-1}^{2nd} = \sqrt{\frac{S_{33}^1 + S_{22}^1 + 2S_{23}^1}{2C_{1212}}}, \quad \lambda_{Sh-2}^{2nd} = \sqrt{\frac{S_{33}^2 + S_{22}^2 - 2S_{23}^2}{2C_{1212}}}, \tag{11}$$

while the extensional characteristic lengths of the second-order continuum are

$$\lambda_{Ext-1}^{2nd} = \sqrt{\frac{S_{11}^{2}}{C_{1111}}}, \quad \lambda_{Ext-2}^{2nd} = \sqrt{\frac{S_{11}^{1}}{C_{2222}}}. \tag{12}$$

According to equations (11-12) the characteristic lengths for the considered RVE are given in Table 4.

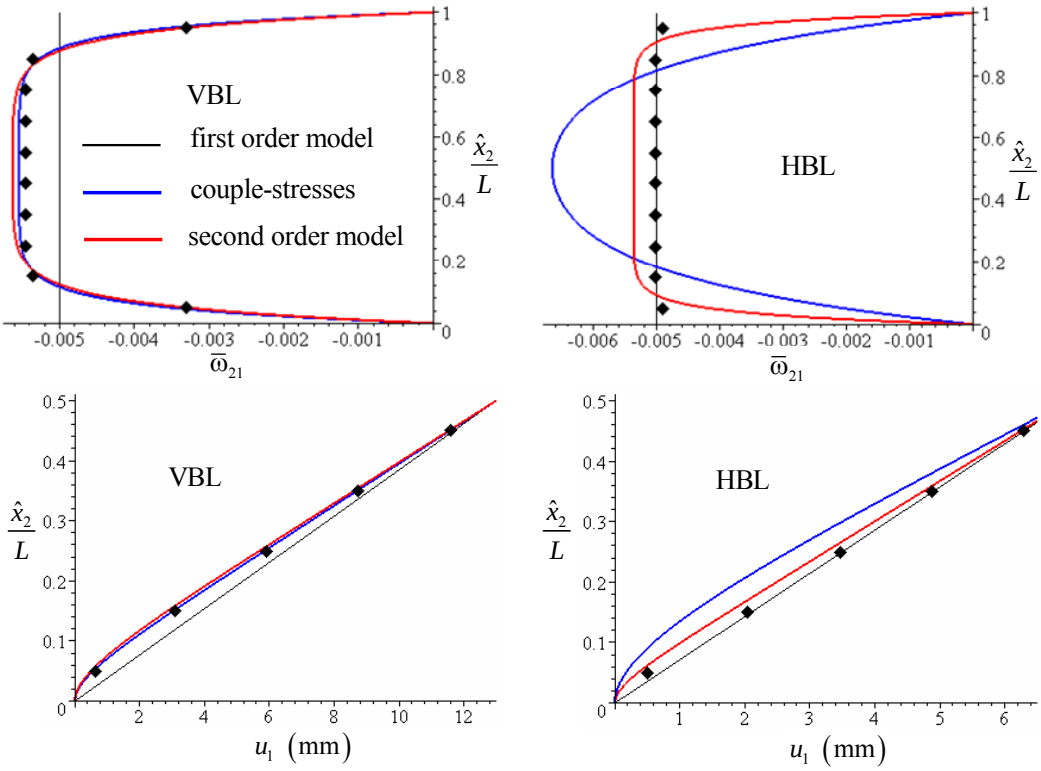


Fig. 4. BSL model: macro-rotation and horizontal displacement at the RVEs from heterogeneous model (diamonds) compared with the macro-rotation field in the homogeneous second order models.

| | *Shear* | | | | | | *Extension* | |
|---|---|---|---|---|---|---|---|---|
| $\boldsymbol{E_b}$ | $\lambda_1^C$ | $\lambda_2^C$ | $\lambda_1^{CS}$ | $\lambda_2^{CS}$ | $\lambda_1^{2nd}$ | $\lambda_2^{2nd}$ | $\lambda_1^{2nd}$ | $\lambda_2^{2nd}$ |
| $10E_m$ | 40 | 68 | 41 | 63 | 104 | 41 | 51 | 14 |
| $10^2 E_m$ | 63 | 84 | 71 | 93 | 124 | 47 | 39 | 16 |
| $10^3 E_m$ | 120 | 182 | 128 | 216 | 147 | 48 | 35 | 20 |

Table 4. Characteristic lengths (mm) (C=Cosserat, CS=Couple-stresses).

The values of the mean tangential traction $t_1$ acting on horizontal planes of the BSL-VBL model (independent on $\hat{x}_2$) evaluated from the different models considered in the present analysis are given in Table 5. Finally, the diagrams in Figure 5 show the ratio of the symmetric part $\overline{\tau}_{(12)}$ and the antisymmetric part $\overline{\tau}_{[12]}$ of the shear stress and the corresponding value $\overline{\tau}_{12}^{1st}$ from the first-order (Cauchy) model.

| ***n*** | $t_1^{FEM}$ (Mpa) | $t_1^{1st}$ (Mpa) | $t_1^{C}$ (Mpa) | $t_1^{CS}$ (Mpa) | $t_1^{2nd}$ (Mpa) |
|---|---|---|---|---|---|
| 6 | 17.0 | 14.7 | 17.3 | 17.6 | 18.1 |
| 10 | 16.3 | 14.7 | 16.1 | 16.3 | 16.5 |

Table 5. Tangential traction at the top edge (1st=Cauchy , C=Cosserat, CS=Couple-stresses).

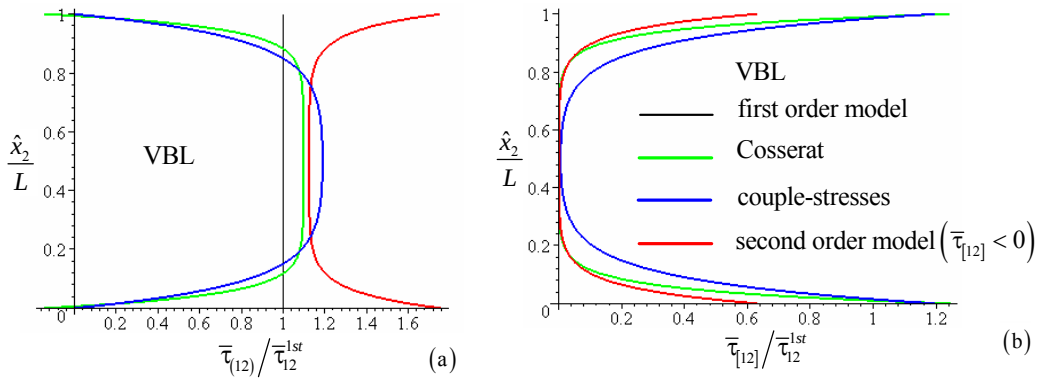


Fig. 5. BSL model: symmetric part (a) and antisymmetric part (b) of the shear stress $\overline{\tau}_{12}$.

## 4 CONCLUSIONS

The in-plane response of elastic periodic masonry has been analyzed with reference to both micro-polar and second-order homogenization techniques. A standard running bond masonry has been considered and the elastic orthotropic moduli have been evaluated according to Cosserat, Couple-stresses and second-order homogenization. A boundary shear layer problem representative of a masonry wall has been analysed to compare the results from the heterogeneous finite element model with the corresponding ones provided by the homogenized continua. The results of the finite element analysis of the heterogeneous model show boundary layer effects when assuming the vertical orientation of the brick layers in the wall. These effects appear to be markedly reduced when the horizontal orientation of the brick layers is considered. The comparison of the results by the homogenised models here considered shows the second-order homogenization technique to be more suitable to describe the sensitivity of the boundary layer effects on the brick layers orientation.

*References*


[1] M. Mistler, A. Anthoine, C. Butenweg, In-plane and out-of-plane homogenisation of masonry, *Computers & Structures*, **85**, 1321-1330, 2007.

[2] P. Trovalusci, R. Masiani, A multifield model for blocky materials based on multiscale description, *Int. J. Solids and Structures*, **42** , 5778-5794, 2005.

[3] J. Sulem, H.B. Mühlhaus, A continuum model for periodic two-dimensional block structures, *Mech. Cohesive-frictional Materials*, **2**, 31-46, 1997.

[4] Salerno G., de Felice G., Continuum modeling of periodic brickwork, *Int. J. Solids and Structures*, **46** ,1251-1267, 2009.

[5] S. Casolo, Macroscopic modelling of structured materials: Relationship between orthotropic Cosserat continuum and rigid elements, *Int. J. Solids and Structures*, **43** ,475-496, 2006.

[6] C. Boutin, Microstructural effects in elastic composites, *Int. J. Solids and Structures*, **33** ,1023-1051, 1996.

[7] N. Triantafyllidis, S. Bardenhagen, The influence od scale size on the stability of periodic solids and the role of associated higher order gradient continuum models, *J. Mechanics and Physiscs of Solids*, **11**, 1891-1928, 1996.

[8] V.P. Smyshlyaev, K.D. Cherednichenko, On rigorous derivation of strain gradient effects in the overall behaviour of periodic heterogeneous media, *J. echanics and Physics of Solids*, **48**, 1325-1357, 2000.

[9] R.H.J. Peerlings, Fleck N.A., Computational Evaluation of Strain Gradient Elasticity Constants, *Int. J. for Multiscale Computational Engineering*, **2**, 599-619, 2004.

[10] F. Bouyge, I. Jasiuk, M. Ostoja-Starzewski, A micromechanically based couple-stress model of an elastic two-phase composite, *Int. J. Solids and Structures*, **38**, 1721-1735, 2001.

[11] F. Bouyge, I. Jasiuk, S. Boccara, M. Ostoja-Starzewski, A micromechanically based couple-stress model of an elastic orthotropic two-phase composite, *European J. of Mechanics A/Solids*, **21**, 465-481, 2002.

[12] S. Forest, K. Sab, Cosserat overall modeling of heterogeneous materials, *Mech. Res. Comm.*, **25**, 449-454, 1998.

[13] L. Gambarotta, A. Bacigalupo, Cosserat homogenization of elastic periodic blocky masonry, in *Proc. 8th World Congress on Computational Mechanics WCCM8*, Venice, 2008.

[14] Ł. Kaczmarczyk, C. Pearce, N. Bićanić, Scale transition and enforcement of RVE boundary conditions in second-order computational homogenization, *Int. J. Numerical Methods in Engineering*, **74**, 506-522, 2008.

[15] V.G. Kouznetsova, M.G.D. Geers, W.A.M. Brekelmans, Multi-scale second-order computational homogenization of multi-phase materials: a nested finite element solution strategy, *Comput. Methods Appl. Mech. Engrg*. **193**, 5525–5550, 2004.